Theranostic Gold Nanoparticles for CT Imaging

Tamar Dreifuss, Eran Barnoy, Menachem Motiei, and Rachela Popovtzer

1   Introduction

One of the major aims in nanomedicine is the ability to perform multiple functions using the same nanovehicle, that is, the ability to achieve both therapeutic and diagnostic imaging capabilities using only a single nanoparticle. The unique physical and optical properties of gold nanoparticles (GNPs), along with the well-known biosafety of gold [1], make GNPs ideal candidates for various biomedical applications, including imaging, therapy, and diagnostic systems. So far, GNPs have been utilized for various therapy applications, such as drug delivery, phototherapy, and radiotherapy, and as a contrast-enhancing agent for computed tomography (CT) and other imaging modalities [2–11]. The wide applications of GNPs and their potential for clinical implementation, as well as the high flexibility in terms of size and shape and the ability to attach multiple types of ligands to their surfaces, have led to varying schemes for developing multifunctional GNPs, with multiple capabilities within a single platform [2, 12, 13]. Compared with other methods, treatment plans involving the use of multifunctional nanoparticles hold the promise of more accurately targeted treatment, with a higher likelihood of a successful outcome. It is this multipronged approach on which many studies have been anchored, since it addresses many issues usually associated with the most aggressive aspects of disease, including multidrug resistance, radioresistance, and recurrence of tumors. Therefore, GNPs have high potential to become the next generation theranostic agents for cancerous diseases. A schematic diagram of potential multifunctional gold nanoparticles for theranostic applications is presented in Fig. 1. This chapter discusses the main approaches for the use of GNPs for both therapy and imaging applications, focusing on multifunctional gold nanoparticles for theranostic applications involving CT imaging.

T. Dreifuss • E. Barnoy • M. Motiei • R. Popovtzer (✉)
Faculty of Engineering and the Institutes of Nanotechnology and Advanced Materials,
Bar-Ilan University, Ramat-Gan, Israel
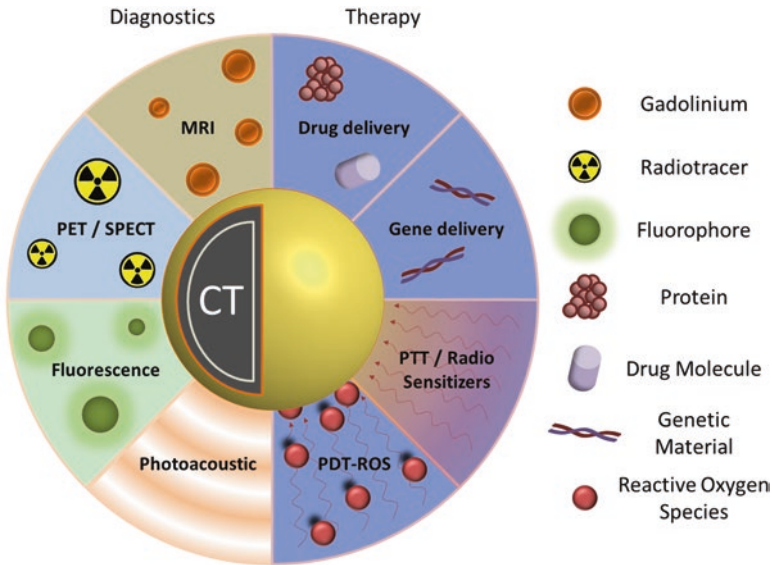e-mail: rachela.popovtzer@biu.ac.il

Fig. 1 Schematic diagram of multifunctional gold nanoparticles (GNPs). Multifunctional GNPs can be prepared by either combining metals with different functionalities or combining functional small-molecules through different surface engineering strategies

2 Gold Nanoparticles as CT Contrast Agents

2.1 Physical Properties

X-ray based CT is among the most convenient imaging/diagnostic tools in hospitals today in terms of availability, efficiency, and cost. CT provides superior visualization of bone structures due to the inherent contrast between electron-dense bones and the more permeable surrounding soft tissues. CT, however, is limited in distinguishing between different soft tissues that have similar densities [14]. CT contrast agents were introduced in order to improve vascular contrast and to enable better delineation of soft tissue structures with similar or identical contrast properties.

Different tissues provide different degrees of X-ray attenuation, according to Eq. (1):

$$I = I_0 e^{-\mu x} \tag{1}$$

where I_0 is the incident X-ray intensity, I is the transmitted X-ray intensity, x is the thickness of the absorber medium, and μ is the mass attenuation coefficient. The most dominant factor impacting the mass attenuation coefficient is the photoelectric effect, which is proportional to the third power of the atomic number of the material (Z^3). Therefore, in order to provide good contrast in CT images, the key factor in the selection of CT contrast agents is high atomic number materials.

Present CT contrast agents are predominantly based on iodine containing molecules, which are effective in absorbing X-rays ($Z=53$). However, the atomic number of gold ($Z=79$) is much higher than that of iodine, and therefore gold can induce stronger X-ray attenuation [15]. The ability of gold to induce high CT contrast was first demonstrated, inadvertently, by Wilhelm Roentgen, in the first medical imaging (Fig. 2). In addition, while iodine containing molecules allow only very short imaging times due to rapid clearance by the kidneys, and are nonspecifically targeted because they cannot be conjugated to most biological components or cancer markers, GNPs can be designed so as to overcome biological barriers and to remain confined to the intravascular space for prolonged times [16–18]. In addition, their strong binding affinity toward thiol, disulfide, and amine groups, enables binding with various targeting agents. Therefore, GNPs are ideal candidates for CT contrast agents. Another advantage of GNPs is their ability to be fabricated in a variety of shapes and sizes, using simple wet-laboratory techniques. Note that for CT imaging the total amount of gold per unit volume (voxel) is the only important parameter regardless of the shape of the particles.

Fig. 2 First ever medical X-ray image (1895) taken by Roentgen. "Hand with Ring" print of Wilhelm Roentgen's first "medical" X-ray, taken on 22 December 1895. It dramatically showed the bones of his wife's fingers; however the real size of her finger's soft tissue could be garnered from the clearly visible gold ring on her finger. Radiology Centennial, Inc. copyrighted in 1993

The high-Z nanoparticle contrast agents could also address the important issue of relatively high radiation exposure of CT. The new generation CT contrast agents that are based on high atomic number materials, such as gold and bismuth, have a great potential not only because of their ability to produce contrast higher than conventional iodine-based contrast agents, but even more importantly, because of the possibility to lower the overall radiation exposure to patients.

Low-to-middle X-ray photon energy (25–120 keV) is used for diagnostic radiology, producing significant contrast between bone and other tissues, resulting in high quality CT images. However, since most of this energy is being absorbed, it exposes the patient to a high dose of radiation. Since the higher energy photons in the energy spectrum produced by the X-ray tubes have a much lower interaction cross section for soft tissue than the nanoparticles, it is possible that filtering lower energies of the X-ray spectrum will lead to lower absorbed radiation dose to the patient. The uptake pattern of these particles can be visualized as distinct contrast relative to their soft tissue background [14]. Therefore, high-Z nanoparticles as contrast agents may permit CT imaging at lower patient doses, with better sensitivity and good specificity.

Spectral CT (popularly referred to as multicolor CT) is a new promising technology that enhances the traditional CT images by using simultaneously different energy settings, which enable the differentiation of materials, based on their energy-related attenuation profiles. The concept of spectral CT exploits the K-edge discontinuity in the photo-electric component of X-ray absorption [19]. Gold has K-edge values within the X-ray energy bandwidth of CT, and thus is an excellent candidate as contrast agents for spectral CT [20]. Several studies have demonstrated that spectral CT can accurately distinguish GNP-based contrast agents from an iodinated contrast agent, tissue, or calcium-rich matter [21–23].

Another important parameter, and indeed a major challenge in the implementation of high-Z contrast agents—lies in the relatively low sensitivity of the CT to the contrast agents' concentration. For example, for MRI contrast agents, proton relaxation must be altered, requiring agents that can perturb the local magnetic field around the proton. The perturbing field in MRI of a super-paramagnetic particle is effective at up to 50-times its diameter, and therefore influences water protons in several cell layers around its location [24]. This phenomenon results in sensitivity of the MRI to micromolar contrast agents' concentration [25]. By contrast, CT contrast agents lack such an amplification ability. CT is sensitive to millimolar contrast agent concentrations; therefore, in order to induce sufficient contrast in the desired organ, a much larger amount of high-Z molecules is needed, since the CT contrast is linearly proportional to the total amount of the high-Z molecules in a voxel.

2.2 GNPs as Blood Pool, Passive and Active Contrast Agents

As blood pool contrast agents, GNPs extended the blood circulation time from several minutes (with the clinically used iodine compounds) to hours or even days [26–29] and show stronger X-ray attenuation than the currently used iodine-based

compounds (under the same clinically relevant conditions) [26, 30]. By taking advantage of the progressive permeation through transendothelial pores on tumor blood vessels (the EPR effect), GNPs of a certain size range can passively accumulate on tumors. This nonselective "passively targeting" approach was demonstrated in several studies which showed significant CT contrast enhancement caused by accumulation of GNPs within the tumor and in areas surrounding it [9, 31].

Conjugation of GNPs to a variety of ligands, including antibodies, peptides, aptamers, or small molecules that possess high affinity toward unique molecular signatures found on diseased cells, produces active targeting agents, which can selectively accumulate on specific cells or tissues. Molecularly targeted nanoparticles reach tumor tissues through the EPR effect (as in passive targeting). However, the active targeting has additive values; the nanoparticles home selectively into specific tumors and remain at the tumor site for extended durations, thereby increasing the local accumulation of the nanoparticles at sites of interest. Studies have shown that molecularly targeted GNPs can enhance the visibility of small tumors in CT, and that active tumor targeting is more efficient than passive targeting [9, 32–34]. This specific interaction between antigen and antibody or receptor and its ligand was shown to be an effective strategy to improve the amount and residence time of contrast agents in tumors, as well as to provide specific molecular knowledge regarding the findings. This new approach of molecularly targeted CT contrast agents has changed the concept of CT from diagnosis based on anatomical structures to diagnosis according to molecular markers.

3 GNP as Multimodal Imaging Contrast Agents

The idea of multimodality imaging, with two or more imaging modalities, has brought new perceptions to the fields of clinical and preclinical imaging. The integration between different individual imaging techniques allows each to compensate for the limitations of the other, thus to achieve synergism and improve the quality and accuracy of the diagnostic tool or research platform. GNPs can be utilized as multimodal imaging contrast agents, for combining CT with additional imaging modalities, as described below.

3.1 CT and MRI

For the development of nanoparticle-based contrast agents for dual mode CT/MR imaging, both CT and MR imaging elements should be incorporated. As the most commonly used MRI contrast agents are based on chelates of gadolinium, gadolinium (Gd)-chelated Au nanoparticles have been designed for CT/MR dual mode imaging in several studies [35–37]. For example, Wen et al. [35] have reported the utilization of gadolinium-loaded dendrimer-entrapped gold nanoparticles (GdeAu DENPs) for

dual mode CT/MR imaging of the heart, liver, kidney, and bladder of rat and mouse. They showed that the GdeAu DENPs have enhanced X-ray attenuation due to the entrapped AuNPs, as well as the complexed Gd(III) ions, which enable efficient dual mode CT/MR imaging. They further showed that the GdeAu DENPs are non-cytotoxic at an Au concentration up to 50 mM, and can be cleared from major organs within 24 h. In another study [36], folic acid-modified multifunctional dendrimer-entrapped gold nanoparticles loaded with gadolinium have been used for targeted CT/MR imaging of cancer in vitro and in vivo via FA receptor-mediated active targeting pathway.

Triple-modal imaging with a single nanostructure has also gained attention in recent years. Hu et al. [37] have developed hybrid gold–gadolinium nanoclusters (NCs), which are suitable for triple-modal NIRF/CT/MRI imaging. The hybrid NCs have been effectively accumulated in tumor tissues and quickly cleared by renal excretion.

3.2 CT and Nuclear Imaging

The incorporation of CT with nuclear imaging (PET and SPECT) enables both functional and anatomical information in a single setting. GNPs can be radiolabeled with different radioactive tracers in order to supplement CT with nuclear imaging. Indeed, coupling of gold to a radiotracer was investigated in a number of studies. A recent study [38] reported the integration of ^{64}Cu into the structures of gold nanoparticles. In this study, PET/CT image of mouse breast cancer model showed high passive tumor targeting and contrast ratios after intravenous injection of those ^{64}CuAuNPs. In another study [39], gold nanocages were prepared and radiolabeled with ^{64}Cu, for evaluating the pharmacokinetics and in vivo cancer targeting capability in a murine EMT-6 breast cancer model. Furthermore, Su et al. [40] have represented theranostic iodine-125-labeled cRGD-gold nanoparticles, which act as tumor-targeted radiosensitizer and SPECT/CT imaging agent. The introduction of ^{125}I on the GNP serves as both a therapeutic factor and a radiotracer for in vivo nuclear imaging. It is important to note that in these aforementioned studies, the use of gold was not aimed to enhance CT intensity, but to earn stability and high loading capabilities of gold nanoparticles, as well as their pharmacokinetics and biodistribution properties.

3.3 CT and Fluorescent Imaging

While optical imaging methods suffer in spatial resolution and offer only a limited penetration depth, they are very sensitive, fast, and readily distinguish between several sources with great soft tissue contrast on cellular and even molecular scales [41–43]. Near-infrared radiation (NIR) allows for relatively deep light penetration into biological tissues with minimal autofluorescence, providing higher signal-to-noise ratios than visible light [41, 43, 44]. A property often used in CT-fluorescence

dual-modal GNP constructs is that GNPs possess very efficient surface-energy transfer properties that can significantly affect the fluorescence of molecules near their surface, both with quenching and with fluorescence enhancement [42, 43, 45–57]. Combining the strong spatial resolution and unlimited penetration depth of CT with the sensitivity available from fluorescence is a promising and widely explored dual-modal imaging technique [42, 43].

Zhang et al. [43] packed gold nanoparticles with a fluorescent dye into polymer micelles. The dye used possessed the unusual property of aggregation-induced emission, so that the aggregated dye was able to produce a signal that overcame the quenching effects of the GNPs. The result was a construct with a strong fluorescent signal, as well as being an efficient CT contrast agent in tumor sites. Sun et al. [58] modified GNPs with glycol chitosan polymers and an NIR fluorescent dye adsorbed using a peptide sequence cleavable by a matrix metalloproteinase (MMP). Prior to cleavage, the GNPs quenched approximately 95 % of the fluorescence compared to the fluorophore alone. Fluorescence was regained proportionally to the concentration of environmental MMP. GNPs allowed easy imaging of the tumor in CT, while the NIR fluorescence signaled strongly starting an hour post injection. Luo et al. [44] attached the NIR dye ICG to gold nanorods coated with mesoporous silica. The layer of silica protected the ICG from GNP quenching. By injecting the constructs into mouse tumors, in addition to the efficient CT images, they witnessed NIR fluorescence up to 12 h post injection. Song et al. [41] coated gold nanospheres with mesoporous silica, and inserted the dye IR-783 into the silica pores. The silica shell was prepared to prevent quenching. In combination, these constructs proved to be strong CT contrast agents with significant fluorescent abilities lasting several hours.

3.4   CT and Photoacoustic Imaging

In photoacoustic (PA) imaging, short laser pulses are delivered into the subject, resulting in local heating which leads to thermoelastic expansion and thus wideband ultrasonic emission. GNPs strongly absorb light and thus are potential contrast agents for PA. The strategy of using GNPs as dual mode CT/PA contrast enhancers has been investigated by Chanda et al. [59]. They used cinnamon-coated gold nanoparticles (Cin-AuNPs) and showed that these particles underwent significant accumulation in breast cancer and prostate cancer cells, facilitating detectable PA signals. In addition, quantitative analysis of CT values in a phantom model revealed that the Cin-AuNPs have reasonable attenuation efficiency. Another recent study, published by Jing et al. [60], has utilized Prussian blue-coated gold nanoparticles (Au@PB NPs) for simultaneous PA/CT bimodal imaging and photothermal ablation of cancer, applying the theranostic approach. The Au@PB NPs were found to be an excellent photoabsorbing agent for both PA imaging and photothermal therapy due to a high photostability and high molar extinction coefficient in NIR region. Moreover, a remarkable enhancement of CT values in tumor sites was observed due to the Au@PB NPs.

4 Therapeutic Gold Nanoparticles

Therapeutic nanoparticles can overcome various limitations of conventional drug delivery systems, such as nonspecific targeting, lack of water solubility, poor oral bioavailability, and low therapeutic indices [16, 61]. GNPs are highly suitable for drug delivery systems, due to their strong binding affinity toward thiol, disulfide, and amine groups, which enables binding with various targeting agents and therapeutic moieties. In addition, by taking advantage of the inherent unique characters of gold itself, GNPs can be exploited to photothermal therapy (PTT) and radiotherapy in which the GNP itself has the therapeutic value, as will be discussed below.

4.1 Drug Delivery

Gold is consistently used in various forms for biological applications owing to ease of fabrication and surface modification, as well as gold's inherent biological compatibility [2, 3, 62, 63]. Using simple wet-laboratory techniques, GNPs have been fabricated in a variety of shapes and sizes, and used as the core or the shell for polymer–metal [62, 63] and metal–metal [64, 65] hybrid nanoparticles. Therapeutics, such as proteins, peptides, oligonucleotides, or small drug molecules, can be attached to the gold nanoparticle surface directly, via amine or thiol groups [63], or indirectly, using a molecule such as bovine serum albumin [66] or the penta-peptide with the amino acid sequence CALNN [67].

GNPs have been widely investigated as drug delivery vehicles for cancer treatment, while implementing both passive and active targeting approaches. For example, a drug delivery system was developed [68] by tethering doxorubicin onto the surface of GNPs with a poly(ethylene glycol) spacer via an acid-labile linkage. The doxorubicin-tethered GNPs (DOX-Hyd@AuNPs) achieved enhanced drug accumulation and retention in multidrug resistant MCF-7/ADR cancer cells when it was compared with free doxorubicin. It released doxorubicin in response to the pH of acidic organelles following endocytosis, and significantly enhanced the cytotoxicity of doxorubicin. Therefore, the DOX-Hyd@AuNPs considerably inhibited the growth of multidrug-resistant MCF-7/ADR cancer cells. In another study [69], the antitumor efficacy of GNPs conjugated non-covalently with three conventional chemotherapy drugs (doxorubicin, cisplatin, and capecitabine) was evaluated in vitro. The cellular proliferation rates in the presence of the anticancer drugs delivered by the GNPs were found to be significantly lower than those of cells exposed to free drugs. In addition, these GNPs were also efficient when tested with chemotherapy resistant cells.

To improve the therapeutic outcomes, the active tumor targeting approach is implemented by coupling targeting agents to drug-loaded GNPs. Prabaharan et al. [70] have synthesized folate (FA)-conjugated amphiphilic GNPs with a poly(L-aspartate-doxorubicin)-b-poly(ethylene glycol) monolayer (Au-P(LA-DOX)-b-PEG-OH/FA) that interacts with the FA receptor. They showed that the presence of FA enables active tumor targeting abilities, as the cellular uptake of the

Au-P(LA-DOX)-b-PEG-OH/FA micelles into cells overexpressing the FA receptor was higher than that of micelles without folate. In addition, Conjugation of DOX onto the NPs and the pH-sensitive properties of its linkage to the NP, greatly reduce the chance of premature drug release during circulation in the bloodstream, offering a potential DOX carrier. In another study [71], Paciotti et al. developed a colloidal GNP that targets the delivery of tumor necrosis factor (TNF) to solid tumors. TNF is an antitumor cytokine that is prone to systemic toxicity when administrated as a free drug. While conjugated to the GNP (which was coated also with PEG-THIOL), it was less toxic and more effective in reducing tumor burden, since maximal antitumor responses in tumor bearing mice were achieved at lower doses of drug. In this study, the TNF served both as antitumor and targeting ligand.

4.2 Gene Delivery

As DNA is not efficiently translocated through the cell membrane [72], designing effective synthetic vectors for transporting nucleic acids, including plasmid DNA, small interfering RNA, or antisense oligonucleotides, is also a challenge which can be addressed using gold nanoparticles [73–76]. Ghosh et al. [77] have demonstrated that coating GNPs with lysine-based headgroups produces effective transfection vectors, without any observed cytotoxicity. They further showed that DNA delivery efficiency strongly depends on the structure of headgroups and their concomitant ability to condense DNA. Importantly, these amino acid-based nanoparticles were responsive to intracellular glutathione levels, during in vitro transfection, providing insight into their mode of activity, as well as a tool for controlled release and concomitant expression of DNA. Guo et al. [78] reported charge-reversal functional GNP as carrier for gene delivery. In this study, Lamin A/C, an important nuclear envelope protein, was effectively silenced by lamin A/C-siRNA delivered by the charge-reversal functional GNPs, whose knockdown efficiency was better than that of commercial Lipofectamine 2000. The charge reversion under an acidic environment facilitated the escape of GNP/nucleic acid complexes from endosome/lysosome and the release of functional nucleic acids into the cytoplasm. Another example of using GNPs for gene silencing was recently presented by Conde et al. [79], who synthesized a library of multifunctional GNPs, aimed to deliver siRNA and specifically silence the c-myc protooncogene. The efficiency of the GNPs was evaluated using a hierarchical approach including three biological systems of increasing complexity (cultured cells, invertebrate, and mammal). After fine-tuning of multiple structural and functional moieties, the most active formulation was selected, consisting of siRNA, which is either covalently or ionically linked to the nanoparticles. Another interesting study [80] has reported proof of concept for the selective release of two different DNA oligonucleotides from two different gold nanorods. DNA was loaded onto the nanorods via thiol conjugation, and selective release was specifically induced by melting of gold nanorods via laser irradiation at the nanorods' longitudinal surface plasmon resonance peaks. The released oligonucleotides remained functional.

4.3 Photothermal Therapy

In the case of photothermal therapy (PTT), GNPs are advantageous because of their ability to strongly absorb light (orders of magnitude higher than organic dye molecules) [3], and then convert the absorbed light into heat via a nonradiative processes. This process occurs on a time scale on the order of picoseconds, leading to intense localized heating and irreparable damage to the cell [81, 82]. In many cases gold by itself has served as the photosensitizer. On the other hand, GNPs enable delivery of exogeneous photosensitizers to cells in high enough concentrations [83]. Moreover, the ability to easily add targeting moieties to the GNP surface enables preferential uptake into the malignant cells, for selective heating of the targeted cells, while leaving the neighboring cells intact.

Consequently, GNPs have been most frequently exploited for PTT, in comparison to options involving other metal, dye–polymer or carbon-based nanoparticles. The exceptionally high extinction coefficient of gold (1×10^{19} M^{-1} cm^{-1} for 20 nm gold nanoparticles) [84] is orders of magnitude higher than that of strongly absorbing organic dyes (e.g., Coomassie blue, 4.3×10^4 M^{-1} cm^{-1}) [85], which makes gold an ideal PTT mediator. Also, the localized surface plasmon resonance of GNPs is highly dependent on the morphology of the nanoparticles and can be easily tuned during the fabrication process [84]. Typically, the absorption of GNPs is tuned to be in the range between 600 and 1000 nm, the so-called therapeutic window in which the interaction of light with biological tissues is low, that is, attenuation and scattering effects are at a minimum.

Nanoparticle-mediated PTT is especially well suited for treating cancer owing to the increased heat sensitivity associated with cancer cells, as well as a tumor's inability to efficiently dissipate heat as a result of its poor vasculature networks. To date, various cancer cell lines, including breast [5], epithelial [86, 87] and colon [12] cancers, have been successfully treated by GNP-mediated PTT, both in vitro and in vivo. Recently, a study that builds on work by Qian et al. [88] has successfully achieved controlled surface engineering of gold nanoparticles, using multiple ligands [PEG 5K, (RGD)4 and NLS (nuclear localization signal) peptides] for efficient delivery into cell nuclei [89]. The nanoparticles were then utilized in PTT studies. One motivation for this study [89] was to investigate the likely advantages of directly heating the nucleus of cancer cells, advantages stemming from the fact that the nucleus has a smaller target volume, a lower heat capacity and an increased likelihood of causing irreparable damage to the cell's DNA. A stark reduction in the survival curves of the cells that had GNPs located predominantly in the nucleus, as opposed to cells that had nanoparticles located predominantly in the cytosol, was observed for cells that were treated under the same conditions, that is, the same GNP concentration and treatment time. Another recent study involving both in vitro and in vivo PTT studies was reported by Yuan et al. [90]. They detailed the fabrication of surfactant-free gold nanostars and their use for both in vitro and in vivo studies of nanoparticle tracking, via plasmon enhanced two-photon photoluminescence, and for PTT of breast cancer cells. Yuan and his colleagues found that 3 min of treatment yielded successful cell kill, and 5 min of treatment gave the best results.

Control measurements involving cells that were exposed to the laser, but had not been incubated with nanostars, showed that these cells were still viable after 5 min of illumination. For the in vivo studies, PEGylated nanostars were injected into CD-1 nude mice that were previously implanted with small dorsal window chambers. After 10 min of PTT, visual confirmation of photo-ablation was indicated by the release of the gold nanoparticles out of the ruptured vessels; scarring occurred 1 week later. One major research area aimed at improving GNP-mediated PTT is the utilization of gold clusters or aggregates [91–94], as the corresponding maximum absorption is red-shifted toward the near-IR range of the "therapeutic window," resulting in less concern regarding unwanted interaction with the surrounding healthy tissues. It should be noted that, despite the multitude of promising outcomes, the variability among the results has continued to encourage further studies aimed at elucidating the mechanisms of heat generation and thermolysis (e.g., shockwaves, micro- and nano-bubbles, and nanoparticle destruction [93, 95, 96]).

4.4 Radiation Therapy

The use of targeted radiosensitizers in cancer treatment is intended to increase tumor sensitivity to radiation, while sparing normal healthy tissue the effects of x-radiation, thereby increasing the therapeutic window. Lately, several studies have suggested that the administration of GNPs into tumors may improve radiosensitivity. GNPs are an ideal candidate to be used as radiosensitizing agents, since high atomic number (Z) materials increase radiation sensitivity owing to their greater absorption of photons and release of secondary energy in the form of photoelectrons, auger electrons, and X-rays into surrounding tissue [30, 97]. The close proximity of GNP to nuclear DNA increases the probability of creating DNA strand breaks, the primary mechanism of radiation-induced cytotoxicity [98, 99]. When GNPs specifically target cancer cells (e.g., via antibody–antigen interaction), large amounts of gold atoms accumulate in the tumor, leading to an enhancement of the radiation effect on the tumor. Chattopadhyay et al. [100] tested the effect of molecularly targeted GNPs on tumor radiosensitization both in vitro and in vivo. In vitro, they combined X-ray exposure with targeted AuNPs (Au-T) and non-targeted AuNPs (Au-P), and found that DNA damage was increased by 1.7- and 3.3-fold in comparison to X-radiation alone, for Au-T and Au-P, respectively. In vivo, the combination of Au-T and X-radiation resulted in regression of human breast cancer tumors by 46 % as compared to treatment with X-radiation. No significant normal tissue toxicity was observed. The mechanism underlying cell death in GNP-induced radiation sensitivity is unclear and several theories have been proposed. The main suggested hypothesis includes an increase in apoptosis, increased generation of intracellular reactive oxygen species or direct DNA damage causing DNA double strand break [98]. Roa et al. [101] found that GNP may sensitize radiotherapy by regulating the cell cycle. They showed that it induced the acceleration of the G0/G1 phase and cell accumulation in the G2/M phase, which were accompanied by downregulation of p53 and cyclin expression and upregulation of cyclin B1 and cyclin E.

4.5 Photodynamic Therapy

Photodynamic therapy (PDT) in cancer treatment involves the uptake of a photosensitizer by cancer tissue followed by photoirradiation [102]. Photoirradiation in the appropriate wavelength excites the photosensitizer to produce reactive oxygen species (ROS), which causes damage to tumor cells. GNPs hold the promise to be highly efficient as photosensitizer carriers, and their use for PDT applications was investigated in several studies. Wieder et al. [103] presented a comparison between silica and gold nanoparticle systems. They argued that photosensitizer-coated GNP is preferable over an encapsulated photosensitizer, in that the generated singlet oxygen would not need to diffuse out of the porous particle structure to elicit cell kill. Hone et al. [104] reported the preparation of GNPs coated with a phthalocyanine (Pc) photosensitizer and their use as delivery vehicle for photodynamic therapy. The nanoparticles, consisted of three components (photosensitizer/gold/phase transfer reagent), were shown to generate singlet oxygen with enhanced quantum yields as compared to the free Pc. In addition, the association of the transfer reagent promoted the solubility of the surface-bound hydrophobic sensitizer in polar solvents, facilitating their systemic injection. In another study, Cheng et al. [105] have developed PEGylated gold nanoparticle conjugates with a reversible PDT drug adsorption, which act as a water-soluble and biocompatible "cage" that allows the delivery of the hydrophobic drug to its site of PDT action. This delivery mode greatly improved the transport of the PDT drug to the tumor relative to conventional drug administration.

5 The Theranostic Approach: Combined Imaging and Therapy

Co-delivery of the above therapeutic and imaging functions by specifically tailored theranostic gold nanosystems can considerably improve medical treatment, particularly in oncology. Diagnosis, treatment, and monitoring response to treatment can be reached with a single approach [5], thus enhancing personalized medicine. We present here prominent recent publications that combine different therapeutic strategies with CT imaging. The data is summarized in Table 1.

5.1 Combining Drug Delivery with CT Imaging

Chemotherapy success requires delivery of drugs to the tumor cells at concentrations above a therapeutic threshold. This is affected not only by the accumulation level in the tumor but also by drug distribution in the tumor stroma, which can often vary among different tumor regions, disease stages, and patients [106]. This issue can be addressed by image-guided drug delivery, which enables monitoring drug distribution in the tumor, as well as in the whole body.

Table 1 Prominent recent studies that combine different therapeutic and diagnostic strategies with CT imaging

Theranostic strategy	Nanoparticle type	Therapeutic agent	Targeting agent	Reference
Drug delivery and CT	Aptamer-conjugated GNP	Dox	PSMA aptamer	[107]
Drug delivery and CT	Dendrimer-entrapped GNP	α-TOS	Folic acid	[108]
Drug delivery and CT	Dendrimer-entrapped GNP	α-TOS	RGD peptide	[113]
PTT and CT	PEG-protected GNR	–	–	[5]
PTT and CT	GNR	–	–	[114]
PTT and CT	Polymer grafted GNP	–	–	[115]
PTT and bimodal SPECT/CT	125I-labeled GNR	–	Folate	[116]
PTT and bimodal PA/CT	PLA microcapsules containing GNPs	–	–	[117]
PTT and bimodal PA/CT	Au@PB core–shell nanoparticle	Prussian blue	–	[60]
PTT and multimodal SERS/CT/TPL	Gold nanostar	–	–	[118]
PTT and multimodal MR/CT/thermal imaging	Fe3O4@Au core–shell nanostar	–	Hyaluronic acid	[119]
RT and CT	PEG-modified GNP	–	–	[120]
RT and CT	Nanogel encapsulating PEGylated GNPs	–	–	[121]
RT and CT	Gold-loaded polymeric micelles	–	–	[122]
RT and bimodal SPECT/CT	125I-labeled GNP	125I	RGD	[40]
RT and bimodal SPECT/CT	131I-labeled GNP	–	C225	[123]
Bimodal RT/PTT and CT	Silica-modified GNR	–	Folic acid	[124]
Multimodal drug delivery/PTT/RT and CT	HGNP	Dox	–	[125]

For this purpose, several studies were conducted in which drugs were loaded onto or into gold nanoparticles for visualization by CT imaging. Kim et al. [107] reported a multifunctional GNP for targeted molecular CT imaging and therapy of prostate cancer. For targeting, the GNP surface was functionalized with a prostate-specific membrane antigen (PSMA) RNA aptamer that binds to PSMA. In vitro experiments showed that the PSMA aptamer-conjugated GNP induced more than fourfold greater CT intensity for a targeted LNCaP cell than that of a nontargeted PC3 cell. Moreover, after loading the targeted GNP with doxorubicin (approximately 615 Dox molecules per GNP), drug release experiments showed that approximately 35 % of Dox was released within 1 h, and the particle potency against targeted LNCaP cells was significantly higher than against nontargeted PC3 cells. Another multifunctional theranostic GNP for targeted CT imaging and drug delivery was developed by Zhu et al. [108]. They reported dendrimer-entrapped GNPs (Au DENPs) covalently linked with α-tocopheryl succinate (α-TOS), which can induce apoptosis of various cancer cells, inhibit the cell cycle, and disrupt the necessary autocrine signaling pathways of tumor growth [109, 110], while not affecting the proliferation of most normal cells [111, 112]. The practical use of free α-TOS is limited due to poor water solubility and bioavailability. In this study, the GNP platform has been found to improve these limitations, without compromising α-TOS therapeutic activity (there was an even higher therapeutic efficacy than that of free α-TOS). Au DENPs were also modified with folic acid (FA) for targeting to cancer cells overexpressing FA receptors (FAR). In vivo experiments with a xenografted tumor model demonstrated that CT images and corresponding CT values of the tumor site did not show an enhancement at 2 h post-injection of both targeted and nontargeted Au DENPs. However, at 24 h post injection, significant CT enhancement in the tumor was observed for mice injected with targeted Au DENPs, compared to that injected with non-targeted Au DENPs (Fig. 3a). In the therapeutic aspect, the tumor growth rate of mice injected with targeted Au DENPs was much slower than that of mice treated with saline, free α-TOS, and non-targeted Au DENPs (Fig. 3b). Following this work, Zhu et al. [113] reported multifunctional Au DENPs, also modified with α-TOS, but with another targeting ligand: arginine–glycine–aspartic acid (RGD) peptide. These multifunctional Au DENPs were able to target cancer cells overexpressing $\alpha_v\beta_3$ integrin and specifically inhibit the growth of the cancer cells. Likewise, via the specific RGD-mediated targeting, $\alpha_v\beta_3$ integrin-overexpressing cancer cells were specifically detected by CT imaging.

5.2 Combining Photothermal Therapy with CT Imaging

The potential of simultaneous utilization of GNPs for CT imaging along with the emerging and highly promising treatment, photothermal therapy, has been widely studied in recent years. Maltzahn et al. [5] developed PEG–protected gold nanorods (PEG-NRs) for both photothermal heat generation and tumor CT imaging. After intra-tumoral administration, Maltzahn et al. fused PEG-NR biodistribution data derived via noninvasive X-ray computed tomography, with four-dimensional computational
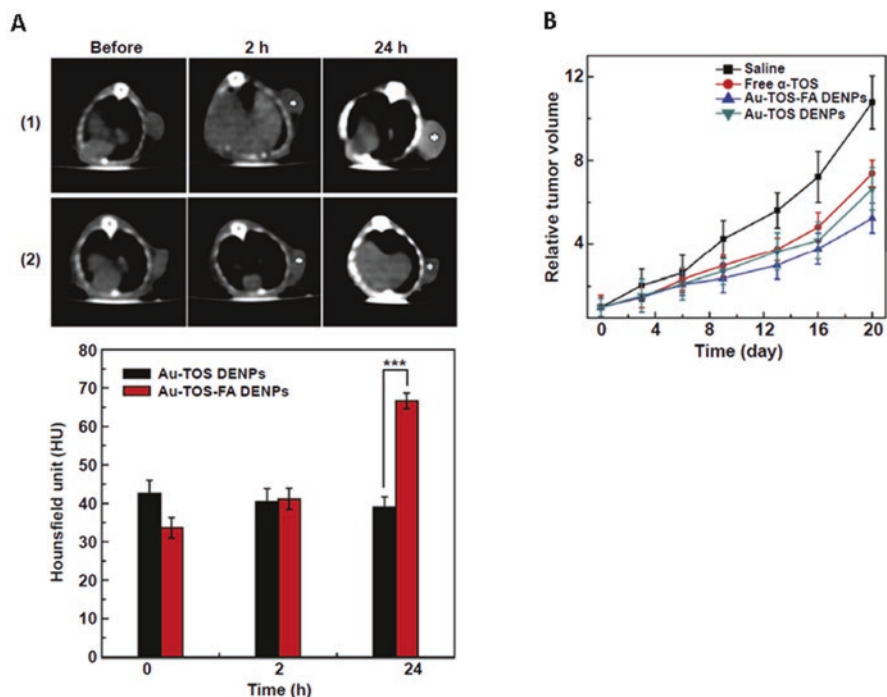
Fig. 3 (**a**) Representative transverse CT images (*top*) and CT values (*bottom*) of U87MG tumor xenografts in nude mice before and after intravenous injection of Au-TOS-FA (1) and Au-TOS (2) DENPs for 2 and 24 h, respectively. The white star indicates the location of the tumor. (**b**) The growth of U87MG xenografted tumors after various treatments. Reprinted with permission from Ref. [108]

heat transport modeling to predict photothermal heating during irradiation. The PEG-NRs exhibited ~2-fold higher X-ray absorption than a clinical iodine contrast agent, and enabled destruction of all irradiated human xenograft tumors in mice. Recently, Qin et al. [114] developed gold nanorods (GNRs) as a theranostic platform for CT imaging and PTT of inflammatory macrophages. In this study, in vitro experiments showed that the GNRs exhibited a significant cell-killing efficacy of macrophages, even at relatively low concentrations of GNRs and low NIR powers. In addition, in vivo therapeutic experiments demonstrated that the GNRs could image and use PTT of inflammatory macrophages in the femoral artery restenosis of an apolipoprotein E knockout (Apo E) mouse model. In another study, Deng et al. [115] presented a gold assembly structure as a potential photothermal therapeutic and CT contrast agent. Two different amphiphilic polymers were anchored onto the GNP, yielding a smart hybrid building block for self-assembly. By varying the ratio of these mixed polymer brushes, a series of amphiphilic nanocrystals was obtained, while an increase in the hydrophobic/hydrophilic ratio resulted in different assembly structures, from a normal monolayer vesicle to large compound micelle (LCM). Due to the strictly packed structure of LCM, the LSPR peaks of GNPs could be tuned to NIR region, for enhanced PTT. In vitro and In vivo studies showed efficient treatment of optimum gold assemblies as a PTT and CT contrast agent (Fig. 4).
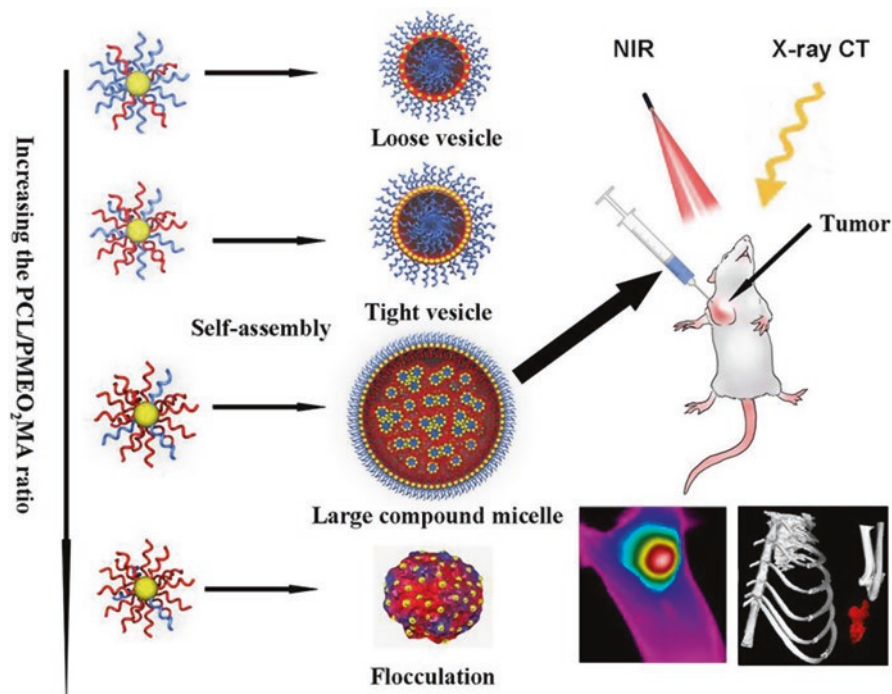
Fig. 4 Schematic representation of assemblies composed by polymer grafted GNPs and their potential application in photothermal therapy and CT imaging of cancer. Reprinted with permission from Ref. [115]

Multifunctional GNPs can serve also for a combination of PTT and multimodal imaging for theranostic applications. For example, incorporation of a radioactive tracer on GNP for dual mode SPECT/CT imaging and PTT was presented by Jang et al. [116]. Likewise, simultaneous photoacoustic/CT bimodal imaging and PTT of cancer using GNPs was presented recently in formulations of graphene oxide modified PLA microcapsules containing gold nanoparticles [117], and core–shell nanoparticles of Au@Prussian blue (Au@PB) [60]. Additional recent studies have demonstrated gold nanostars (GNS) as theranostic probes for PTT and multimodal imaging of cancer [118, 119].

5.3   Combining Radiation Therapy with CT Imaging

Image-guided RT (IGRT) relies on the ability to localize tumors in order to optimize the therapeutic outcomes. GNPs may represent an efficient theranostic adjuvant for CT-guided RT treatment, due to their radiosensitive properties and the ability to enhance CT contrast. Accordingly, they are currently being studied in this theranostic role, and have thus far shown great potential in clinical applications. Joh et al. [120]

have investigated the therapeutic and diagnostic value of PEG-modified GNPs (P-GNPs) combined with RT for sarcoma. Their experimental techniques included intravenous administration of the P-GNP, CT imaging of mice with engrafted sarcoma tumors for RT treatment planning, and precision-targeted RT delivered using a Small Animal Radiation Research Platform (SARRP). The results demonstrated that P-GNP in conjunction with RT enhanced CT imaging, caused increased RT-induced DNA damage, and led to significantly reduced clonogenic survival of tumor cells, compared to RT alone, while minimizing radiation dose to normal tissues. Jølck et al. [121] have developed a nanogel based on colloidal gold in a sucrose acetate isobutyrate gelating matrix, for IGRT. They investigated the induced CT contrast and the stability of the nanogel over a period of 12 weeks. It was demonstrated that once injected, the nanogel remained at the injection site and provided excellent CT-contrast as visualized by micro-CT imaging. In addition, in vitro and in vivo experiments showed that the nanogel was stable over time both in terms of geometry, volume, and GNP content. Minor degradation was observed after 12 weeks, suggesting an acceptable degradation profile for image guidance in patients undergoing fractioned RT, as the treatment is typically conducted within a 6 weeks time frame. Another nanoplatform that could simultaneously generate a CT image contrast and serve as a radiosensitizer was developed by Zaki et al. [122]. They prepared gold-loaded polymeric micelles (GPMs), which provided blood pool contrast for up to 24 h following intravenous injection, and improved the delineation of tumor margins via CT. In combination of GPMs with radiation, tumor-bearing mice exhibited a 1.7-fold improvement in the median survival time compared with mice receiving radiation alone (Fig. 5).

Multifunctional theranostic GNPs for combination of RT with dual-mode SPECT/CT were also presented by Su et al. [40], who used targeted ^{125}I-labeled cRGD-GNPs, and by Kao et al. [123], who used ^{131}I-labeled EGFR-targeted GNPs.

5.4   Combining Multimodal Therapy with CT Imaging

Today, treating patients with a broad-spectrum approach is preferable among most clinicians. Multimodal therapy (MMT) combines different therapeutic strategies to improve treatment outcomes. GNPs have been investigated in several studies as both CT contrast agents and MMT enhancers. Huang et al. [124] have designed a multifunctional nanoprobe of folic acid-conjugated silica-modified GNR with the aim of investigating the feasibility of their use as X-ray/CT imaging-guided targeting dual-mode RT and PTT. The prepared nanoprobes showed highly selective targeting, enhanced RT and PTT effects on MGC803 gastric cancer cells, and also exhibited strong X-ray attenuation for in vivo X-ray and CT imaging. In another study, Park et al. [125] have reported multifunctional hollow GNPs (HGNP) designed for triple combination therapy and CT imaging. The shell thickness of HGNPs can tune the surface plasmon resonance to the near infrared light, resulting in a photothermal ablation of tumors, whereas the hollow cavity within a HGNP is able to accommodate a high payload of chemotherapeutic agents. This study utilized HGNPs for CT imaging and combined drug delivery (of doxorubicin), thermal

Fig. 5 (**a**) Representative CT images in the axial plane prior to injection (precontrast) and 30 min, 24 h, and 48 h postinjection of GPMs or AuroVist (individual 1.9 nm GNPs). Tumor boundaries are indicated by *white arrows*. (**b**) Quantitative analysis of CT images. (**c**) Kaplan-Meier survival analysis for tumor-bearing mice receiving no treatment (*dotted gray line*), GPMs only (*dotted black line*), irradiation only (*solid gray line*), or irradiation 24 h after retro-orbital injection of GPMs (*solid black line*). Reprinted with permission from Ref. [122]
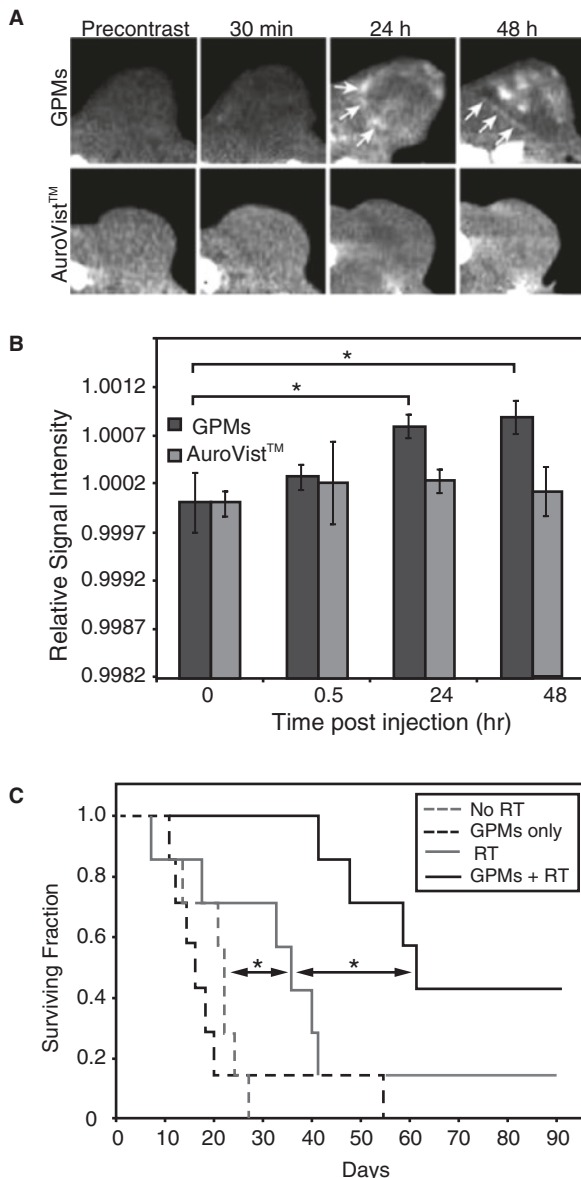
therapy, and radiotherapy. Synthesized Dox-HGNPs exhibited better response to radiation for CT imaging and cancer therapy. It was shown also that Dox-HGNPs were capable of triggering Dox release by NIR laser, converting light to heat for photothermal ablation and enhancing radiosensitization of the tumor. In vivo experiments showed that the triple treatment effects of Dox, heat, and radiation dramatically enhanced tumor growth delay by a factor of 4.3.

6 Conclusions and Future Perspectives

The aforementioned studies, both for imaging and therapy, demonstrate that GNPs are highly favorable candidates for various therapeutic and diagnostic implementations, each one separately, or together in a multimodal approach. Furthermore, the unique physicochemical properties of GNPs, along with their biocompatibility and low toxicity, have led to excellent performance in the few clinical trials involving GNPs [126]. In the theranostic field, which is based on the "all-in-one" approach, the broad possible range of structures, hybridizations, coatings, and capacities marks GNPs as the next generation of theranostic agents. The concept of theranostics with multifunctional GNPs has a great potential to enhance the medical area towards personalized medicine. However, a broad and thorough evaluation of the long-term toxicity of GNPs is still required in order to translate them to the clinic.

References

1. Connor EE, Mwamuka J, Gole A, Murphy CJ, Wyatt MD. Gold nanoparticles are taken up by human cells but do not cause acute cytotoxicity. Small. 2005;1:325–7. doi:10.1002/smll.200400093.
2. Boisselier E, Astruc D. Gold nanoparticles in nanomedicine: preparations, imaging, diagnostics, therapies and toxicity. Chem Soc Rev. 2009;38:1759. doi:10.1039/b806051g.
3. Jain S, Hirst DG, O'Sullivan JM. Gold nanoparticles as novel agents for cancer therapy. Br J Radiol. 2012;85:101–13. doi:10.1259/bjr/59448833.
4. Sean Norman R, Stone JW, Gole A, Murphy CJ, Sabo-Attwood TL. Targeted photothermal lysis of the pathogenic bacteria, pseudomonas aeruginosa, with gold nanorods. Nano Lett. 2008;8:302–6. doi:10.1021/nl0727056.
5. Von Maltzahn G, Park J-H, Agrawal A, Bandaru NK, Das SK, Sailor MJ, et al. Computationally guided photothermal tumor therapy using long-circulating gold nanorod antennas. Cancer Res. 2009;69:3892–900. doi:10.1158/0008-5472.CAN-08-4242.
6. Minati L, Antonini V, Torrengo S, Serra MD, Boustta M, Leclercq X, et al. Sustained in vitro release and cell uptake of doxorubicin adsorbed onto gold nanoparticles and covered by a polyelectrolyte complex layer. Int J Pharm. 2012;438:45–52. doi:10.1016/j.ijpharm.2012.08.057.
7. Rand D, Ortiz V, Liu Y, Derdak Z, Wands JR, Tatíček M, et al. Nanomaterials for X-ray imaging: gold nanoparticle enhancement of X-ray scatter imaging of hepatocellular carcinoma. Nano Lett. 2011;11:2678–83. doi:10.1021/nl200858y.
8. Popovtzer R, Agrawal A, Kotov NA, Popovtzer A, Balter J, Carey TE, et al. Targeted gold nanoparticles enable molecular CT imaging of cancer. Nano Lett. 2008;8:4593–6. doi:10.1021/nl8029114.
9. Popovtzer R. Targeted gold nanoparticles enable molecular CT imaging of cancer: an in vivo study. Int J Nanomed. 2011;6:2859. doi:10.2147/IJN.S25446.
10. Jakobsohn K, Motiei M, Sinvani M, Popovtzer R. Towards real-time detection of tumor margins using photothermal imaging of immune-targeted gold nanoparticles. Int J Nanomed. 2012;7:4707–13. doi:10.2147/IJN.S34157.
11. Shilo M, Reuveni T, Motiei M, Popovtzer R. Nanoparticles as computed tomography contrast agents: current status and future perspectives. Nanomedicine. 2012;7:257–69. doi:10.2217/nnm.11.190.
12. Huang H-C, Barua S, Sharma G, Dey SK, Rege K. Inorganic nanoparticles for cancer imaging and therapy. J Control Release. 2011;155:344–57. doi:10.1016/j.jconrel.2011.06.004.

13. Liu D, Wang Z, Jiang X. Gold nanoparticles for the colorimetric and fluorescent detection of ions and small organic molecules. Nanoscale. 2011;3:1421–33. doi:10.1039/c0nr00887g.

14. Yu S, Watson AD, Bismuth B. Metal-based X-ray contrast media. 1999.

15. Xu C, Tung GA, Sun S. Size and concentration effect of gold nanoparticles on X-ray attenuation as measured on computed tomography. Chem Mater. 2008;20:4167–9. doi:10.1021/cm8008418.

16. Petros RA, DeSimone JM. Strategies in the design of nanoparticles for therapeutic applications. Nat Rev Drug Discov. 2010;9:615–27. doi:10.1038/nrd2591.

17. Hallouard F, Anton N, Choquet P, Constantinesco A, Vandamme T. Iodinated blood pool contrast media for preclinical X-ray imaging applications—a review. Biomaterials. 2010;31:6249–68. doi:10.1016/j.biomaterials.2010.04.066.

18. Allkemper T, Bremer C, Matuszewski L, Ebert W, Reimer P. Contrast-enhanced blood-pool MR angiography with optimized iron oxides: effect of size and dose on vascular contrast enhancement in rabbits. Radiology. 2002;223:432–8. doi:10.1148/radiol.2232010241.

19. Schirra CO, Brendel B, Anastasio MA, Roessl E. Spectral CT: a technology primer for contrast agent development. Contrast Media Mol Imaging 9:62–70. doi: 10.1002/cmmi.1573.

20. Pan D, Roessl E, Schlomka J-P, Caruthers SD, Senpan A, Scott MJ, et al. Computed tomography in color: NanoK-enhanced spectral CT molecular imaging. Angew Chem Int Ed. 2010;49:9635–9. doi:10.1002/anie.201005657.

21. Cormode DP, Roessl E, Thran A, Skajaa T, Gordon RE, Schlomka J-P, et al. Atherosclerotic plaque composition: analysis with multicolor CT and targeted gold nanoparticles. Radiology. 2010;256:774–82. doi:10.1148/radiol.10092473.

22. Schirra CO, Senpan A, Roessl E, Thran A, Stacy AJ, Wu L, et al. Second generation gold nanobeacons for robust K-edge imaging with multi-energy CT. J Mater Chem. 2012;22:23071–7. doi:10.1039/C2JM35334B.

23. Roessl E, Cormode D, Brendel B, Jürgen Engel K, Martens G, Thran A, et al. Preclinical spectral computed tomography of gold nano-particles. Nucl Instruments Methods Phys Res Sect A Accel Spectrometers Detect Assoc Equip. 2011;648:S259–64. doi:10.1016/j.nima.2010.11.072.

24. Wolf GL. Magnetic resonance imaging and the future of cardiac imaging. Am J Cardiol. 1989;64:E60–3. doi:10.1016/0002-9149(89)90736-4.

25. Skotland T, Iversen T-G, Sandvig K. New metal-based nanoparticles for intravenous use: requirements for clinical success with focus on medical imaging. Nanomed Nanotechnol Biol Med. 2010;6:730–7. doi:10.1016/j.nano.2010.05.002.

26. Kojima C, Umeda Y, Ogawa M, Harada A, Magata Y, Kono K. X-ray computed tomography contrast agents prepared by seeded growth of gold nanoparticles in PEGylated dendrimer. Nanotechnology. 2010;21:245104. doi:10.1088/0957-4484/21/24/245104.

27. Kim D, Park S, Lee JH, Jeong YY, Jon S. Antibiofouling polymer-coated gold nanoparticles as a contrast agent for in vivo X-ray computed tomography imaging. J Am Chem Soc. 2007;129:7661–5. doi:10.1021/ja071471p.

28. Cai Q-Y, Kim SH, Choi KS, Kim SY, Byun SJ, Kim KW, et al. Colloidal gold nanoparticles as a blood-pool contrast agent for X-ray computed tomography in mice. Invest Radiol. 2007;42:797–806. doi:10.1097/RLI.0b013e31811ecdcd.

29. Peng C, Zheng L, Chen Q, Shen M, Guo R, Wang H, et al. PEGylated dendrimer-entrapped gold nanoparticles for in vivo blood pool and tumor imaging by computed tomography. Biomaterials. 2012;33:1107–19. doi:10.1016/j.biomaterials.2011.10.052.

30. Hainfeld JF, Slatkin DN, Focella TM, Smilowitz HM. Gold nanoparticles: a new X-ray contrast agent. Br J Radiol. 2006;79:248–53. doi:10.1259/bjr/13169882.

31. Ghaghada KB, Badea CT, Karumbaiah L, Fettig N, Bellamkonda RV, Johnson GA, et al. Evaluation of tumor microenvironment in an animal model using a nanoparticle contrast agent in computed tomography imaging. Acad Radiol. 2011;18:20–30. doi:10.1016/j.acra.2010.09.003.

32. Hainfeld JF, O'Connor MJ, Dilmanian FA, Slatkin DN, Adams DJ, Smilowitz HM. Micro-CT enables microlocalisation and quantification of Her2-targeted gold nanoparticles within tumour regions. Br J Radiol. 2014.

33. Chanda N, Kattumuri V, Shukla R, Zambre A, Katti K, Upendran A, et al. Bombesin functionalized gold nanoparticles show in vitro and in vivo cancer receptor specificity. Proc Natl Acad Sci U S A. 2010;107:8760–5. doi:10.1073/pnas.1002143107.

34. Wang H, Zheng L, Peng C, Shen M, Shi X, Zhang G. Folic acid-modified dendrimer-entrapped gold nanoparticles as nanoprobes for targeted CT imaging of human lung adencarcinoma. Biomaterials. 2013;34:470–80. doi:10.1016/j.biomaterials.2012.09.054.

35. Wen S, Li K, Cai H, Chen Q, Shen M, Huang Y, et al. Multifunctional dendrimer-entrapped gold nanoparticles for dual mode CT/MR imaging applications. Biomaterials. 2013;34:1570–80. doi:10.1016/j.biomaterials.2012.11.010.

36. Chen Q, Li K, Wen S, Liu H, Peng C, Cai H, et al. Targeted CT/MR dual mode imaging of tumors using multifunctional dendrimer-entrapped gold nanoparticles. Biomaterials. 2013;34:5200–9. doi:10.1016/j.biomaterials.2013.03.009.

37. Hu D-H, Sheng Z-H, Zhang P-F, Yang D-Z, Liu S-H, Gong P, et al. Hybrid gold–gadolinium nanoclusters for tumor-targeted NIRF/CT/MRI triple-modal imaging in vivo. Nanoscale. 2013;5:1624. doi:10.1039/c2nr33543c.

38. Zhao Y, Sultan D, Detering L, Cho S, Sun G, Pierce R, et al. Copper-64-alloyed gold nanoparticles for cancer imaging: improved radiolabel stability and diagnostic accuracy. Angew Chem Int Ed. 2014;53:156–9. doi:10.1002/anie.201308494.

39. Wang Y, Liu Y, Luehmann H, Xia X, Brown P, Jarreau C, et al. Evaluating the pharmacokinetics and in vivo cancer targeting capability of au nanocages by positron emission tomography imaging. ACS Nano. 2012;6:5880–8. doi:10.1021/nn300464r.

40. Su N, Dang Y, Liang G, Liu G. Iodine-125-labeled cRGD-gold nanoparticles as tumor-targeted radiosensitizer and imaging agent. Nanoscale Res Lett. 2015;10:160. doi:10.1186/s11671-015-0864-9.

41. Song J-T, Yang X-Q, Zhang X-S, Yan D-M, Wang Z-Y, Zhao Y-D. Facile synthesis of gold nanospheres modified by positively charged mesoporous silica, loaded with near-infrared fluorescent dye, for in vivo X-ray computed tomography and fluorescence dual mode imaging. ACS Appl Mater Interfaces. 2015;7:17287–97. doi:10.1021/acsami.5b04359.

42. Sun I-C, Eun D-K, Koo H, Ko C-Y, Kim H-S, Yi DK, et al. Tumor-targeting gold particles for dual computed tomography/optical cancer imaging. Angew Chem. 2011;123:9520–3. doi:10.1002/ange.201102892.

43. Zhang J, Li C, Zhang X, Huo S, Jin S, An F-F, et al. In vivo tumor-targeted dual-modal fluorescence/CT imaging using a nanoprobe co-loaded with an aggregation-induced emission dye and gold nanoparticles. Biomaterials. 2015;42:103–11. doi:10.1016/j.biomaterials.2014.11.053.

44. Luo T, Huang P, Gao G, Shen G, Fu S, Cui D, et al. Mesoporous silica-coated gold nanorods with embedded indocyanine green for dual mode X-ray CT and NIR fluorescence imaging. Opt Express. 2011;19:17030. doi:10.1364/OE.19.017030.

45. Lee D-E, Koo H, Sun I-C, Ryu JH, Kim K, Kwon IC. Multifunctional nanoparticles for multimodal imaging and theragnosis. Chem Soc Rev. 2012;41:2656–72. doi:10.1039/c2cs15261d.

46. Lee S, Cha E-J, Park K, Lee S-Y, Hong J-K, Sun I-C, et al. A near-infrared-fluorescence-quenched gold-nanoparticle imaging probe for in vivo drug screening and protease activity determination. Angew Chemie. 2008;120:2846–9. doi:10.1002/ange.200705240.

47. Razgulin A, Ma N, Rao J. Strategies for in vivo imaging of enzyme activity: an overview and recent advances. Chem Soc Rev. 2011;40:4186–216. doi:10.1039/c1cs15035a.

48. Cheng W, Chen Y, Yan F, Ding L, Ding S, Ju H, et al. Ultrasensitive scanometric strategy for detection of matrix metalloproteinases using a histidine tagged peptide-Au nanoparticle probe. Chem Commun (Camb). 2011;47:2877–9. doi:10.1039/c0cc04441e.

49. Park SY, Lee SM, Kim GB, Kim Y-P. Gold nanoparticle-based fluorescence quenching via metal coordination for assaying protease activity. Gold Bull. 2012;45:213–9.

50. Tira DS, Focsan M, Ulinici S, Maniu D, Astilean S. Rhodamine B-coated gold nanoparticles as effective "turn-on" fluorescent sensors for detection of Zinc II ions in water. Spectrosc Lett. 2013;47:153–9. doi:10.1080/00387010.2013.782557.

51. Hutter E, Maysinger D. Gold-nanoparticle-based biosensors for detection of enzyme activity. Trends Pharmacol Sci. 2013;34:497–507. doi:10.1016/j.tips.2013.07.002.

52. Mohamed MB, Volkov V, Link S, El-sayed MA. The "lightning" gold nanorods: fluorescence enhancement of over a million compared to the gold metal. Chem Phys Lett. 2000;317:517–23.

53. Geddes C, Lakowicz J. Metal-enhanced fluorescence. J Fluoresc. 2002;12:121–9.

54. Ming T, Zhao L, Yang Z, Chen H, Sun L, Wang J, et al. Strong polarization dependence of plasmon-enhanced fluorescence on single gold nanorods. Nano Lett. 2009;9:3896–903. doi:10.1021/nl902095q.

55. Abadeer N, Brennan M, Wilson W, Murphy C. Distance and plasmon wavelength dependent fluorescence of molecules bound to silica-coated gold nanorods. ACS Nano. 2014;8:8392–406.

56. Kang K, Wang J. Conditionally activating optical contrast agent with enhanced sensitivity via gold nanoparticle plasmon energy transfer: feasibility study. J Nanobiotechnology. 2014;12:56. doi:10.1186/s12951-014-0056-2.

57. Kang KA, Wang J. Smart dual-mode fluorescent gold nanoparticle agents. Wiley Interdiscip Rev Nanomed Nanobiotechnol. 2014;6:398–409. doi:10.1002/wnan.1267.

58. Sun I-C, Eun D-K, Koo H, Ko C-Y, Kim H-S, Yi DK, et al. Tumor-targeting gold particles for dual computed tomography/optical cancer imaging. Angew Chem Int Ed Engl. 2011;50:9348–51. doi:10.1002/anie.201102892.

59. Chanda N, Shukla R, Zambre A, Mekapothula S, Kulkarni RR, Katti K, et al. An effective strategy for the synthesis of biocompatible gold nanoparticles using cinnamon phytochemicals for phantom CT imaging and photoacoustic detection of cancerous cells. Pharm Res. 2011;28:279–91. doi:10.1007/s11095-010-0276-6.

60. Jing L, Liang X, Deng Z, Feng S, Li X, Huang M, et al. Prussian blue coated gold nanoparticles for simultaneous photoacoustic/CT bimodal imaging and photothermal ablation of cancer. Biomaterials. 2014;35:5814–21. doi:10.1016/j.biomaterials.2014.04.005.

61. Cho K, Wang X, Nie S, Chen ZG, Shin DM. Therapeutic nanoparticles for drug delivery in cancer. Clin Cancer Res. 2008;14:1310–6. doi:10.1158/1078-0432.CCR-07-1441.

62. Beija M, Li Y, Duong HT, Laurent S, Elst LV, Muller RN. Polymer–gold nanohybrids with potential use in bimodal MRI/CT: enhancing the relaxometric properties of Gd(iii) complexes. J Mater Chem. 2012;22:21382. doi:10.1039/c2jm34999j.

63. Xie M, Ding L, You Z, Gao D, Yang G, Han H. Robust hybrid nanostructures comprising gold and thiol-functionalized polymer nanoparticles: facile preparation, diverse morphologies and unique properties. J Mater Chem. 2012;22:14108. doi:10.1039/c2jm31228j.

64. Han S-Y, Guo Q-H, Xu M-M, Yuan Y-X, Shen L-M, Yao J-L, et al. Tunable fabrication on iron oxide/Au/Ag nanostructures for surface enhanced Raman spectroscopy and magnetic enrichment. J Colloid Interface Sci. 2012;378:51–7. doi:10.1016/j.jcis.2012.04.047.

65. Guo X, Zhang Q, Sun Y, Zhao Q, Yang J. Lateral etching of core–shell Au@Metal nanorods to metal-tipped Au nanorods with improved catalytic activity. ACS Nano. 2012;6:1165–75. doi:10.1021/nn203793k.

66. Tkachenko AG, Xie H, Liu Y, Coleman D, Ryan J, Glomm WR, et al. Cellular trajectories of peptide-modified gold particle complexes: comparison of nuclear localization signals and peptide transduction domains. Bioconjug Chem. 2004;15:482–90. doi:10.1021/bc034189q.

67. Nativo P, Prior IA, Brust M. Uptake and intracellular fate of surface-modified gold nanoparticles. ACS Nano. 2008;2:1639–44. doi:10.1021/nn800330a.

68. Wang F, Wang YC, Dou S, Xiong MH, Sun TM, Wang J. Doxorubicin-tethered responsive gold nanoparticles facilitate intracellular drug delivery for overcoming multidrug resistance in cancer cells. ACS Nano. 2011;5:3679–92. doi:10.1021/nn200007z.

69. Tomuleasa C, Soritau O, Orza A, Dudea M, Petrushev B, Mosteanu O, et al. Gold nanoparticles conjugated with cisplatin/doxorubicin/capecitabine lower the chemoresistance of hepatocellular carcinoma-derived cancer cells. J Gastrointest Liver Dis. 2012;21:188–96.

70. Prabaharan M, Grailer JJ, Pilla S, Steeber DA, Gong S. Gold nanoparticles with a monolayer of doxorubicin-conjugated amphiphilic block copolymer for tumor-targeted drug delivery. Biomaterials. 2009;30:6065–75. doi:10.1016/j.biomaterials.2009.07.048.

71. Paciotti GF, Myer L, Weinreich D, Goia D, Pavel N, McLaughlin RE, et al. Colloidal gold: a novel nanoparticle vector for tumor directed drug delivery. Drug Deliv. 2004;11:169–83. doi:10.1080/10717540490433895.

72. Sokolova V, Epple M. Inorganic nanoparticles as carriers of nucleic acids into cells. Angew Chemie Int Ed. 2008;47:1382–95. doi:10.1002/anie.200703039.

73. Han G, Ghosh P, De M, Rotello VM. Drug and gene delivery using gold nanoparticles. NanoBiotechnology. 2007;3:40–5. doi:10.1007/s12030-007-0005-3.

74. Chen C-C, Lin Y-P, Wang C-W, Tzeng H-C, Wu C-H, Chen Y-C, et al. DNA-gold nanorod conjugates for remote control of localized gene expression by near infrared irradiation. J Am Chem Soc. 2006;128:3709–15. doi:10.1021/ja0570180.

75. Kim J-H, Yeom J-H, Ko J-J, Han MS, Lee K, Na S-Y, et al. Effective delivery of anti-miRNA DNA oligonucleotides by functionalized gold nanoparticles. J Biotechnol. 2011;155:287–92. doi:10.1016/j.jbiotec.2011.07.014.

76. Shan Y, Luo T, Peng C, Sheng R, Cao A, Cao X, et al. Gene delivery using dendrimer-entrapped gold nanoparticles as nonviral vectors. Biomaterials. 2012;33:3025–35. doi:10.1016/j.biomaterials.2011.12.045.

77. Ghosh PS, Kim C-K, Han G, Forbes NS, Rotello VM. Efficient gene delivery vectors by tuning the surface charge density of amino acid-functionalized gold nanoparticles. ACS Nano. 2008;2:2213–8. doi:10.1021/nn800507t.

78. Guo S, Huang Y, Jiang Q, Sun Y, Deng L, Liang Z, et al. Enhanced gene delivery and siRNA silencing by gold nanoparticles coated with charge-reversal polyelectrolyte. ACS Nano. 2010;4:5505–11. doi:10.1021/nn101638u.

79. Conde J, Ambrosone A, Sanz V. Design of multifunctional gold nanoparticles for in vitro and in vivo gene silencing. ACS Nano. 2012;6(9):8316–24.

80. Wijaya A, Schaffer SB, Pallares IG, Hamad-Schifferli K. Selective release of multiple DNA oligonucleotides from gold nanorods. ACS Nano. 2009;3:80–6. doi:10.1021/nn800702n.

81. Link S, El-Sayed MA. Spectral properties and relaxation dynamics of surface plasmon electronic oscillations in gold and silver nanodots and nanorods. J Phys Chem B. 1999;103:8410–26. doi:10.1021/jp9917648.

82. El-Sayed MA. Some interesting properties of metals confined in time and nanometer space of different shapes. Acc Chem Res. 2001;34:257–64. doi:10.1021/ar960016n.

83. Curry T, Epstein T, Smith R, Kopelman R. Photothermal therapy of cancer cells mediated by blue hydrogel nanoparticles. Nanomedicine. 2013;8:1577–86. doi:10.2217/nnm.12.190.

84. Link S, El-Sayed MA. Shape and size dependence of radiative, non-radiative and photothermal properties of gold nanocrystals. Int Rev Phys Chem. 2010.

85. Chial HJ, Thompson HB, Splittgerber AG. A spectral study of the charge forms of Coomassie blue G. Anal Biochem. 1993;209:258–66. doi:10.1006/abio.1993.1117.

86. Choi J, Yang J, Bang D, Park J, Suh J-S, Huh Y-M, et al. Targetable gold nanorods for epithelial cancer therapy guided by near-IR absorption imaging. Small. 2012;8:746–53. doi:10.1002/smll.201101789.

87. El-Sayed IH, Huang X, El-Sayed MA. Selective laser photo-thermal therapy of epithelial carcinoma using anti-EGFR antibody conjugated gold nanoparticles. Cancer Lett. 2006;239:129–35. doi:10.1016/j.canlet.2005.07.035.

88. Qian W, Murakami M, Ichikawa Y, Che Y. Highly efficient and controllable PEGylation of gold nanoparticles prepared by femtosecond laser ablation in water. J Phys Chem C. 2011;115:23293–8. doi:10.1021/jp2079567.

89. Curry TY. Nanoparticles for biomedical applications: photothermal therapy and nuclear delivery. 2013.

90. Yuan H, Khoury CG, Wilson CM, Grant GA, Bennett AJ, Vo-Dinh T. In vivo particle tracking and photothermal ablation using plasmon-resonant gold nanostars. Nanomed Nanotechnol Biol Med. 2012;8:1355–63. doi:10.1016/j.nano.2012.02.005.

91. Zharov VP, Galitovskaya EN, Johnson C, Kelly T. Synergistic enhancement of selective nanophotothermolysis with gold nanoclusters: potential for cancer therapy. Lasers Surg Med. 2005;37:219–26. doi:10.1002/lsm.20223.

92. Nam J, Won N, Jin H, Chung H, Kim S. pH-Induced aggregation of gold nanoparticles for photothermal cancer therapy. J Am Chem Soc. 2009;131:13639–45. doi:10.1021/ja902062j.

93. Hühn D, Govorov A, Gil PR, Parak WJ. Photostimulated Au nanoheaters in polymer and biological media: characterization of mechanical destruction and boiling. Adv Funct Mater. 2012;22:294–303. doi:10.1002/adfm.201101134.

94. Murthy AK, Stover RJ, Borwankar AU, Nie GD, Gourisankar S, Truskett TM, et al. Equilibrium gold nanoclusters quenched with biodegradable polymers. ACS Nano. 2013;7:239–51. doi:10.1021/nn303937k.

95. Letfullin RR, Joenathan C, George TF, Zharov VP. Laser-induced explosion of gold nanoparticles: potential role for nanophotothermolysis of cancer. Nanomedicine. 2006;1:473–80. doi:10.2217/17435889.1.4.473.

96. Coronado EA, Encina ER, Stefani FD. Optical properties of metallic nanoparticles: manipulating light, heat and forces at the nanoscale. Nanoscale. 2011;3:4042–59. doi:10.1039/c1nr10788g.

97. Hainfeld JF, Slatkin DN, Smilowitz HM. The use of gold nanoparticles to enhance radiotherapy in mice. Phys Med Biol. 2004;49:N309–15. doi:10.1088/0031-9155/49/18/N03.

98. De Jong WH, Hagens WI, Krystek P, Burger MC, Sips AJ, Geertsma RE. Particle size-dependent organ distribution of gold nanoparticles after intravenous administration. Biomaterials. 2008;29:1912–9. doi:10.1016/j.biomaterials.2007.12.037.

99. Hainfeld JF, Dilmanian FA, Slatkin DN, Smilowitz HM. Radiotherapy enhancement with gold nanoparticles. J Pharm Pharmacol. 2008;60:977–85. doi:10.1211/jpp.60.8.0005.

100. Chattopadhyay N, Cai Z, Kwon YL, Lechtman E, Pignol JP, Reilly RM. Molecularly targeted gold nanoparticles enhance the radiation response of breast cancer cells and tumor xenografts to X-radiation. Breast Cancer Res Treat. 2013;137:81–91. doi:10.1007/s10549-012-2338-4.

101. Roa W, Zhang X, Guo L, Shaw A, Hu X, Xiong Y, et al. Gold nanoparticle sensitize radiotherapy of prostate cancer cells by regulation of the cell cycle. Nanotechnology. 2009;20:375101. doi:10.1088/0957-4484/20/37/375101.

102. Bechet D, Couleaud P, Frochot C, Viriot M-L, Guillemin F, Barberi-Heyob M. Nanoparticles as vehicles for delivery of photodynamic therapy agents. Trends Biotechnol. 2008;26:612–21. doi:10.1016/j.tibtech.2008.07.007.

103. Wieder ME, Hone DC, Cook MJ, Handsley MM, Gavrilovic J, Russell DA. Intracellular photodynamic therapy with photosensitizer-nanoparticle conjugates: cancer therapy using a "Trojan horse". Photochem Photobiol Sci. 2006;5:727–34. doi:10.1039/b602830f.

104. Hone D, Walker P, Evans-Gowing R. Generation of cytotoxic singlet oxygen via phthalocyanine-stabilized gold nanoparticles: a potential delivery vehicle for photodynamic therapy. Langmuir. 2002;2985–7. doi: 10.1021/la0256230.

105. Cheng Y, Samia AC, Meyers JD, Panagopoulos I, Fei B, Burda C. Highly efficient drug delivery with gold nanoparticle vectors for in vivo photodynamic therapy of cancer. J Am Chem Soc. 2008;130:10643–7. doi:10.1021/ja801631c.

106. Bao G, Mitragotri S, Tong S. Multifunctional nanoparticles for drug delivery and molecular imaging. Annu Rev Biomed Eng. 2013;15:253–82. doi:10.1146/annurev-bioeng-071812-152409.

107. Kim D, Jeong YY, Jon S. A drug-loaded aptamer-gold nanoparticle bioconjugate for combined CT imaging and therapy of prostate cancer. ACS Nano. 2010;4:3689–96. doi:10.1021/nn901877h.

108. Zhu J, Zheng L, Wen S, Tang Y, Shen M, Zhang G, et al. Targeted cancer theranostics using alpha-tocopheryl succinate-conjugated multifunctional dendrimer-entrapped gold nanoparticles. Biomaterials. 2014;35:7635–46. doi:10.1016/j.biomaterials.2014.05.046.

109. Won Y-W, Yoon S-M, Lim KS, Kim Y-H. Self-assembled nanoparticles with dual effects of passive tumor targeting and cancer-selective anticancer effects. Adv Funct Mater. 2012;22:1199–208. doi:10.1002/adfm.201101979.

110. Won Y-W, Yoon S-M, Sonn CH, Lee K-M, Kim Y-H. Nano self-assembly of recombinant human gelatin conjugated with α-tocopheryl succinate for Hsp90 inhibitor, 17-AAG, delivery. ACS Nano. 2011;5:3839–48. doi:10.1021/nn200173u.

111. Gogvadze V, Norberg E, Orrenius S, Zhivotovsky B. Involvement of Ca2+ and ROS in α-tocopheryl succinate-induced mitochondrial permeabilization. Int J Cancer. 2010;127:1823–32. doi:10.1002/ijc.25204.

112. Prasad KN, Kumar B, Yan X-D, Hanson AJ, Cole WC. α-tocopheryl succinate, the most effective form of vitamin E for adjuvant cancer treatment: a review. J Am Coll Nutr. 2003;22:108–17. doi:10.1080/07315724.2003.10719283.

113. Zhu J, Fu F, Xiong Z, Shen M, Shi X. Dendrimer-entrapped gold nanoparticles modified with RGD peptide and alpha-tocopheryl succinate enable targeted theranostics of cancer cells. Colloids Surf B Biointerfaces. 2015;133:36–42. doi:10.1016/j.colsurfb.2015.05.040.

114. Qin J, Peng Z, Li B, Ye K, Zhang Y, Yuan F, et al. Gold nanorods as a theranostic platform for in vitro and in vivo imaging and photothermal therapy of inflammatory macrophages. Nanoscale. 2015;7:13991–4001. doi:10.1039/C5NR02521D.

115. Deng H, Zhong Y, Du M, Liu Q, Fan Z, Dai F, et al. Theranostic self-assembly structure of gold nanoparticles for NIR photothermal therapy and X-Ray computed tomography imaging. Theranostics. 2014;4:904–18. doi:10.7150/thno.9448.

116. Jang B, Park S, Kang SH, Kim JK, Kim S-K, Kim I-H, et al. Gold nanorods for target selective SPECT/CT imaging and photothermal therapy in vivo. Quant Imaging Med Surg. 2012;2:1–11. doi:10.3978/.issn.2223-4292.2012.01.03.

117. Jin Y, Wang J, Ke H, Wang S, Dai Z. Graphene oxide modified PLA microcapsules containing gold nanoparticles for ultrasonic/CT bimodal imaging guided photothermal tumor therapy. Biomaterials. 2013;34:4794–802. doi:10.1016/j.biomaterials.2013.03.027.

118. Liu Y, Ashton JR, Moding EJ, Yuan H, Register JK, Fales AM, et al. A plasmonic gold nanostar theranostic probe for in vivo tumor imaging and photothermal therapy. Theranostics. 2015;5:946–60. doi:10.7150/thno.11974.

119. Li J, Hu Y, Yang J, Wei P, Sun W, Shen M, et al. Hyaluronic acid-modified Fe3O4@Au core/shell nanostars for multimodal imaging and photothermal therapy of tumors. Biomaterials. 2015;38:10–21. doi:10.1016/j.biomaterials.2014.10.065.

120. Joh DY, Kao GD, Murty S, Stangl M, Sun L, Al Zaki A, et al. Theranostic gold nanoparticles modified for durable systemic circulation effectively and safely enhance the radiation therapy of human sarcoma cells and tumors. Transl Oncol. 2013;6:722–31. doi:10.1593/tlo.13433.

121. Jølck RI, Binderup T, Hansen AE, Scherman JB, Munch AF, Rosenschold P, Kjaer A, et al. Injectable colloidal gold in a sucrose acetate isobutyrate gelating matrix with potential use in radiation therapy. Adv Healthc Mater. 2014;3:1680–7. doi:10.1002/adhm.201300668.

122. Al Zaki A, Joh D, Cheng Z, De Barros ALB, Kao G, Dorsey J, et al. Gold-loaded polymeric micelles for computed tomography-guided radiation therapy treatment and radiosensitization. ACS Nano. 2014;8:104–12. doi:10.1021/nn405701q.

123. Kao HW, Lin YY, Chen CC, Chi KH, Tien DC, Hsia CC, et al. Evaluation of EGFR-targeted radioimmuno-gold-nanoparticles as a theranostic agent in a tumor animal model. Bioorg Med Chem Lett. 2013;23:3180–5. doi:10.1016/j.bmcl.2013.04.002.

124. Huang P, Bao L, Zhang C, Lin J, Luo T, Yang D, et al. Folic acid-conjugated silica-modified gold nanorods for X-ray/CT imaging-guided dual-mode radiation and photo-thermal therapy. Biomaterials. 2011;32:9796–809. doi:10.1016/j.biomaterials.2011.08.086.

125. Park J, Park J, Ju EJ, Park SS, Choi J, Lee JH, et al. Multifunctional hollow gold nanoparticles designed for triple combination therapy and CT imaging. J Control Release. 2015;207:77–85. doi:10.1016/j.jconrel.2015.04.007.

126. Pillai G. Nanomedicines for cancer therapy: an update of FDA approved and those under various stages of development. SOJ Pharm Pharm Sci. 2014;1:13.